Superconducting pairing mediated by spin fluctuations from first principles

F. Essenberger,[1] A. Sanna,[1] A. Linscheid,[1] F. Tandetzky,[1] G. Profeta,[2] P. Cudazzo,[3,4] and E. K. U. Gross[1]

[1]*Max Planck Institute of Microstructure Physics, Weinberg 2, D-06120 Halle, Germany*
[2]*Consiglio Nazionale delle Ricerche-Superconducting and Innovative Materials and Devices (CNR-SPIN), 67100 L'Aquila, Italy*
[3]*Nano-Bio Spectroscopy Group, Departamento Física de Materiales, Universidad del País Vasco, Centro de Física de Materiales*
CSIC-UPV/EHU-MPC and DIPC, Avenida Tolosa 72, E-20018 San Sebastián, Spain
[4]*European Theoretical Spectroscopy Facility (ETSF)*

We present the derivation of an *ab initio* and parameter-free effective electron-electron interaction that goes beyond the screened random phase approximation and accounts for superconducting pairing driven by spin fluctuations. The construction is based on many-body perturbation theory and relies on the approximation of the exchange-correlation part of the electronic self-energy within time-dependent density functional theory. This effective interaction is included in an exchange-correlation kernel for superconducting density functional theory in order to achieve a completely parameter free superconducting gap equation. First results from applying the new functional to a simplified two-band electron gas model are consistent with experiments.

I. INTRODUCTION

In the last 30 y the field of superconductivity has been revolutionized by the discovery of high-temperature (hi-T_c) superconductivity (SC). First the cuprates were found in the 1980s [1,2] and then iron-based compounds in the 2000s [3–5]. Numerous theoretical models have been developed in order to grasp the essential physics of these materials [6–8] and still the community is far from a general consensus on the origin of the pairing mechanism. In our opinion, consensus can only be achieved in one single way: by developing a universal predictive theory of (hi-T_c) SC that is fully parameter free and is able to reproduce the essential properties of the SC (including its critical temperature, complex gap function, and excitation spectrum), using only the knowledge of the atomic constituents and chemical structure.

Within the class of conventional (meaning phonon-driven) SC, density functional theory for the SC state (SCDFT) [9], within the available functional [10,11], proved to be predictive and reliable [12–21]. However, since the pairing in the pnictides and cuprates is nonphononic [22,23], this SCDFT approach is not directly applicable, due to the limitations of the functional.

In this work we carefully reconsider this functional and its construction, in particular the treatment of the electronic component of the pairing. We aim to reach two goals in this work. The *first* is very general and not bound to SCDFT applications. We want to formulate a screened effective electron-electron interaction that goes beyond the GW form and includes additional physical effects not present in the random phase approximation (RPA) type of screening. In particular we aim to include the effect of low-energy spin fluctuations in a computationally feasible way and completely *ab initio* (i.e., without the use of parameters, like a Stoner exchange splitting). We focus on the spin fluctuations because they are one of the prime candidates responsible for SC pairing in iron SC [24]. The *second* goal we aim for is to cast this effective interaction along the standard Coulomb and phonon contribution [10] in a functional that can be used within the *ab initio* SCDFT framework.

From several empirical/semiempirical calculations [25], where all three interactions are included, it is, in fact, known that the interplay between the different pairing channels leads to a strong competition and to several interesting physical effects. The paper has the following outline. In the next section (Sec. II) we discuss briefly the existing functionals of SCDFT. Then we propose the set of relevant diagrams for representing the spin fluctuations (Sec. III A) and the corresponding self-energy contributions are constructed in the Nambu formalism (Sec. III B). After some additional approximation (Sec. III C), the final form of the self-energy taking the spin fluctuations into account is presented in Sec. IV. This self-energy may be used also in many-body theory but the focus of this work lies on SCDFT and hence in Sec. V a functional is derived using the Sham-Schlüter connection. In the last part of the present work (Sec. VI) the functional is applied to a two-band model system and the trends with respect to the Coulomb, phonon and spin-fluctuation (SF) contributions are investigated.

II. A BRIEF REVIEW OF SCDFT

Before engaging in the task of constructing the effective interaction and the corresponding functional, we briefly review the SCDFT framework and the available functionals. SCDFT is based on a theorem of Oliveira, Gross, and Kohn [9], that extends the Hohenberg-Kohn proof [26] of the 1:1 correspondence between density and external potential to the SC density,

$$\chi(\boldsymbol{r},\boldsymbol{r}') = \langle \hat{\Psi}_\downarrow(\boldsymbol{r})\hat{\Psi}_\uparrow(\boldsymbol{r}')\rangle,$$

where $\hat{\Psi}_\sigma(\boldsymbol{r})$ are the usual electronic field operators and $\langle \cdots \rangle$ is the thermal average. The modern version of the theory has been reformulated by Lüders, Marques, and co-workers [10,18]. This formulation includes an explicit ionic density and a further extension of the Hohenberg-Kohn proof in the spirit of the multicomponent DFT introduced by Kreibich and Gross [27].

In their work, Lüders, Marques, and co-workers [10,18] proposed an exchange-correlation functional derived from many-body perturbation theory and presented solutions of the

SC Kohn-Sham (KS) system for real SC. The starting point is an approximation for the self-energy. In their work they use

$$\bar{\Sigma}_k(\omega_n) \approx \sum_m \sum_{k'} W_{kk'}(\omega_n - \omega_m) \bar{G}^{KS}_{k'}(\omega_m) \qquad (1)$$

$$+ \sum_m \sum_{k'} \Lambda^{Ph}_{kk'}(\omega_n - \omega_m) \bar{G}^{KS}_{k'}(\omega_m), \qquad (2)$$

where $\bar{G}^{KS}_k(\omega_n)$ is the Green's function of the SC KS system in Nambu notation [28], $W_{kk'}(\omega_n)$ is the screened Coulomb interaction, and $\Lambda^{Ph}_{kk'}$ is the interaction mediated by phonons. We indicate objects in Nambu notation with a bar (for example $\bar{G}$). The components of the Green's function read

$$\bar{G}_k(\omega_n) = \tau^z \begin{pmatrix} G_k(\omega_n) & F_k(\omega_n) \\ F^{\dagger}_k(\omega_n) & G^{\dagger}_k(\omega_n) \end{pmatrix}, \qquad (3)$$

where the ω_n are the fermionic Matsubara frequencies, k is a combined index $k = \{n\bm{k}\}$ containing the band index and the momentum of the KS electron, and τ^z is the third Pauli matrix. The normal (G_k) and anomalous (F_k) parts of the Nambu Green's function are given by

$$G_k(\omega_n) = -\int_0^\beta d\tau\, e^{i\omega_n\tau} \langle \hat{T}[\hat{a}_k(\tau)\hat{a}^{\dagger}_k(0)]\rangle,$$

$$F_k(\omega_n) = -\int_0^\beta d\tau\, e^{i\omega_n\tau} \langle \hat{T}[\hat{a}_k(\tau)\hat{a}_k(0)]\rangle,$$

where $\hat{a}_k(\tau)$ and $\hat{a}^{\dagger}_k$ are the usual creation and annihilation operators in the Heisenberg picture, $\hat{T}$ is the time ordering operator, and $\langle \cdots \rangle$ denotes the thermal average. The electronic part of the interaction, in the work of Marques and Lüders, is assumed to be given by the classical (test charge to test charge) screened Coulomb interaction [29]; therefore, it can be expressed in terms of the dielectric function ϵ^{-1},

$$W_{k_1 k_2}(\omega_n) = \sum_{k'} \epsilon^{-1}_{k_1 k'}(\omega_n) v_{k' k_2}, \qquad (4)$$

where $v_{k_1 k_2}$ is the bare Coulomb interaction. The interaction mediated by phonons $\Lambda^{Ph}_{kk'}(\omega_n)$ depends on the electron-phonon coupling matrix elements $g^{kk'}_{\lambda\bm{q}}$ and the phonon frequencies $\Omega_{\lambda\bm{q}}$:

$$\Lambda^{Ph}_{kk'}(\omega_n) = -\frac{1}{\pi} \int_0^\infty d\omega \frac{2\omega}{\omega_n^2 + \omega^2} \mathrm{Im}\big[\Lambda^{Ph}_{kk'}(\omega)\big],$$

$$\mathrm{Im}\big[\Lambda^{Ph}_{kk'}(\omega)\big] = -\pi \sum_{\lambda\bm{q}} \big|g^{kk'}_{\lambda\bm{q}}\big|^2 \delta(\omega - \Omega_{\lambda\bm{q}}). \qquad (5)$$

A Feynman diagram schematic form for this approximation is shown in Eq. (6). For the two terms we use the names $\bar{\Sigma}^{GW}$ and $\bar{\Sigma}^{Ph}$, respectively:

$$(6)$$

Once an approximation for the self-energy is fixed, it is possible to construct the corresponding exchange-correlation (xc) potential using the Sham-Schlüter connection (see Sec. V for details). A key approximation in order to reduce the numerical complexity of SCDFT is the so-called decoupling approximation [30], i.e.,

$$\Delta^{xc}_{kk'} \approx \delta_{kk'} \Delta^{xc}_k,$$

which can be interpreted as the exclusion of hybridization effects between the non-SC KS orbitals by the effect of the SC condensation. In this approximation the electronic KS system can be diagonalized analytically, leading to a self-consistent expression for the pairing potential Δ^{xc}_k known as the SCDFT gap equation,

$$\Delta^{xc}_k = -\Delta^{xc}_k \mathcal{Z}^D_k - \sum_{k'} \mathcal{K}^C_{kk'} \frac{\tanh\left(\frac{\beta E_{k'}}{2}\right)}{2E_{k'}} \Delta^{xc}_{k'}, \qquad (7)$$

that has the BCS form [31]. The kernels $\mathcal{Z}^D_k$ and $\mathcal{K}^C_{kk'}$ depend on the temperature, the interaction matrix elements $\big(w_{k_1 k_2}, \Lambda^{Ph}_{kk'}\big)$, the single-particle KS energies ϵ_k and $E_k := \sqrt{|\Delta_k|^2 + (\epsilon_k - \mu)^2}$. The critical temperatures predicted within this equation agree extremely well with the experimentally observed ones within the class of phononic SC [12–15,18,21,32,33]. However, Eq. (7) fails to describe hi-T_c SC [5,34], where the SC mechanism is believed to be related to magnetic interactions.

In the next sections we see that this fact is actually not surprising. One assumption in using a dielectric type of electron-electron interaction is that all vertex corrections in the Coulomb part of the self-energy are completely neglected. As one can see in Eq. (6), by comparing the approximation with its exact counterpart obtained from Hedin's equations [35]. Vertex corrections can be safely disregarded in the phonon-related part of the self-energy (at least within the domain of validity of Migdal's theorem [36]), but are crucial to account for magnetic fluctuation effects, which are discussed in the next sections.

III. EXTENSION OF THE SELF-ENERGY

In this section we construct a form of the self-energy containing the relevant processes involved in a SF-mediated pairing. The effective interaction is evaluated in the parent metallic system in which SC takes place (i.e., we ignore the feedback effect of the SC condensation). This approximation may not be valid at low temperature where the condensation strongly affects the screening of magnetic fluctuations [6,37,38]. However, this assumption is exact near the critical point since the SC phase transition is of the continuous, second-order type. Therefore, the approximation will not affect the estimation of a critical temperature.
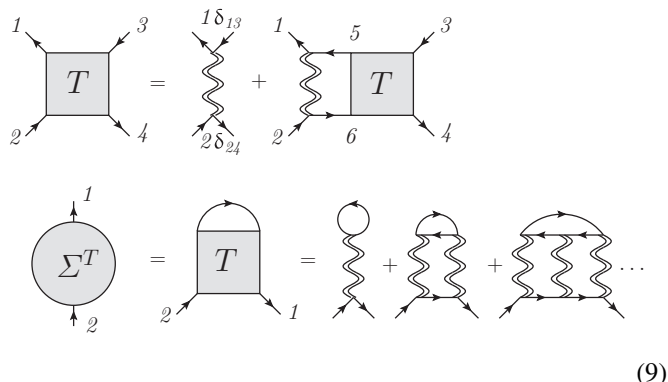
Note, that the same approximation was applied to the phononic part of the interaction, entering the gap equation [Eq. (7)]. In this case the effect of the condensation on the pairing strength is most likely negligible even at low temperature [39,40].

A. Inclusion of the relevant diagrams

To go beyond the GW approximation, we consider [41] the T matrix [42–44], which is given by a Bethe-Salpeter equation (BSE) [45]:
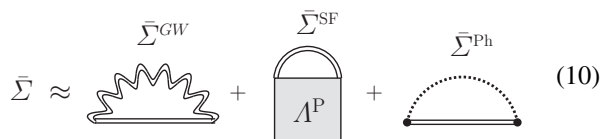
$$T(1,2,3,4) = w(1,3)\,\delta_{13}\delta_{24}$$
$$+ w(1,2)\,G(1,5)\,G(2,6)\,T(5,6,3,4). \quad (8)$$

The coordinate 1 is a compact notation: $1 = \{\boldsymbol{r}_1, \tau_1, \sigma_1\}$, where $\boldsymbol{r}_1$ is the real space vector, τ_1 the Matsubara time, and σ_1 the spin index. The diagrammatic form of this BSE and the self-energy contribution $\bar{\Sigma}^T = \bar{G}T$ corresponding to the T matrix are shown in Eq. (9).

$$(9)$$

Empirically, it is well known that the response function in the T-matrix approximation leads to reasonable results for the magnetic response function [43,44]. $\bar{\Sigma}^T$ has been used in various studies to account for magnetic fluctuations in non-SC systems [46–49].
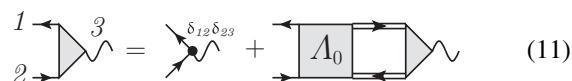
However, for reasons that we discuss in Sec. III C, we do not make direct use of the T matrix and the corresponding self-energy for constructing the effective interaction. Instead we consider a larger set of diagrams, by starting from the particle-hole propagator Λ^P [50–52]. This object contains all proper particle-hole contributions. These are all diagrams which are irreducible with respect to a bare Coulomb interaction and have two incoming and two outgoing open coordinates. The T matrix is fully contained in Λ^P. We use the analogy with $\bar{\Sigma}^T$ [see Eq. (9)], to formulate the self-energy containing magnetic fluctuations as

$$(10)$$

In Eq. (10) we only show a simple diagrammatic form, details are derived explicitly in the next section. Note that this form of the self-energy contains both Hartree and xc contributions, while only the xc parts enter the functional derivative appearing in the vertex part of Hedin's equations. The Hartree contribution is implicitly removed in Sec. III C when we define the approximation for Λ^P. Also double-counting problems related to this choice of the self-energy are addressed in Sec. III C. As a general convention in this work, we always refer to the xc (Hartree-free) part of the self-energy.

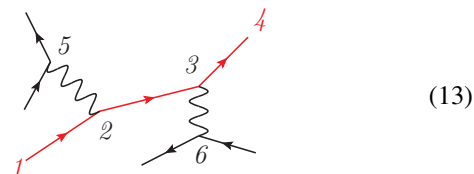### B. Properties of the particle-hole propagator

In this section we investigate the properties of the particle-hole propagator, which is the key object of our derivation. For simplicity we restrict ourselves to collinear magnetic systems; i.e., we assume a spin-diagonal Green's function $G(1,2) = \delta_{\sigma_1\sigma_2} G(1,2)$. One of Hedin's equations is a Dyson equation for the vertex $\Gamma(1,2,3)$,

$$(11)$$

where the kernel of the Dyson equation is given by

$$\Lambda_0(1,2,3,4) := \frac{\delta\Sigma^V(1,2)}{\delta G(3,4)} \quad (12)$$

and is called an irreducible particle-hole propagator [52]. The Λ_0 contains all connected diagrams which are irreducible with respect to a bare Coulomb interaction and the particle-hole propagator. The coordinates 1 and 4 are connected to outgoing Green's functions and 2 and 3 to incoming ones. [Eq. (16)]. The self-energy used in the construction of the kernel is indicated by Σ^V. The kernel Λ_0 also plays the central role in the BSE equation for Λ^P, which we derive now. However, before this can be done it is necessary to classify the two possible contributions present in Λ_0. The distinction between the two sets is made using the concept of a path. A path is a chain of Green's function lines connecting to coordinates. For example, in Eq. (13), we have a path connecting the coordinates 1 and 4:

$$(13)$$

After this definition we can introduce the two possible contribution present in Λ_0.

(1) The crossed contribution Λ_0^c, which has a path connecting the coordinates $1 \leftrightarrow 3$ and $2 \leftrightarrow 4$. The spin contributions in this set are

$$\Lambda_0^c(1,2,3,4) \equiv \delta_{\sigma_1\sigma_3}\delta_{\sigma_2\sigma_4}\Lambda_0^c(1,2,3,4). \quad (14)$$

Note that the contributions to the T matrix [Eq. (9)] are all of this type [43].

(2) The direct contribution Λ_0^d, which has a path connecting the coordinates $1 \leftrightarrow 2$ and $3 \leftrightarrow 4$. The spin contributions in this set are

$$\Lambda_0^d(1,2,3,4) \equiv \delta_{\sigma_1\sigma_2}\delta_{\sigma_3\sigma_4}\Lambda_0^d(1,2,3,4). \quad (15)$$

The kernels Λ_0^c and Λ_0^d are created by the functional derivative of the self-energy with respect to G. By the functional derivative $\frac{\delta}{\delta G(3,4)}$ one Green's function within the self-energy is removed and the open connections get the indices 3 and 4

resulting in the four-point function $\Lambda_0(1,2,3,4)$.

(16)

If the removed function was part of a loop, the resulting contribution is direct. It is crossed otherwise [Eq. (16)]. Since a loop was destroyed in the derivative, an extra minus sign is necessary to compensate for this:

$$\Lambda_0^c(1,2,3,4) = \frac{\delta \Sigma^V(1,2)}{\delta G(3,4)} \text{ with } G \text{ not in loop,} \quad (17)$$

$$\Lambda_0^d(1,2,3,4) = -\frac{\delta \Sigma^V(1,2)}{\delta G(3,4)} \text{ with } G \text{ in loop.} \quad (18)$$

It is important to keep track for these *signs* since, while Feynman diagrams have an explicit sign convention, symbolic expressions [like the ones written in terms of the particle-hole propagator Eq. (10)] do not.

Due to Eqs. (12), (17), and (18), the total irreducible particle-hole propagator is given by the difference between the crossed and direct contributions:

$$\Lambda_0(1,2,3,4) = \frac{\delta \Sigma^V(1,2)}{\delta G(3,4)} = \Lambda_0^c - \Lambda_0^d =: \Lambda_0^{c-d}. \quad (19)$$

With these preliminary considerations we can start to derive a BSE for Λ^P. Note that also within the set Λ^P all contributions are either direct or crossed, i.e., $\Lambda^P = \Lambda^c + \Lambda^d$. If, for example, two crossed contribution are linked, the resulting one stays crossed.

(20)

Any other combination leads to a direct contribution. A special case is the connection of two direct contributions, in

which a loop is created:

(21)

Considering these cases, the BSEs for the direct and crossed contribution of the particle-hole propagator read

$$\Lambda^P = \sum_{n=0}^{\infty} \Lambda_{(n)}^c + \sum_{n=0}^{\infty} \Lambda_{(n)}^d,$$

$$\Lambda_{(n+1)}^c = \Lambda_0^c GG \Lambda_{(n)}^c, \quad (22)$$

$$\Lambda_{(n+1)}^d = \Lambda_0^d GG \Lambda_{(n)}^c + \Lambda_0^c GG \Lambda_{(n)}^d - \Lambda_0^d GG \Lambda_{(n)}^d, \quad (23)$$

where (n) labels the order in the irreducible particle-hole propagator and the zero order $\Lambda_{(0)}^{c,d}$ is given by the irreducible part $\Lambda_0^{c,d}$. By subtracting Eqs. (22) and (23) we find a combined BSE for Λ^{c-d} containing crossed and direct terms:

$$\Lambda^{c-d} = \Lambda_0 + \Lambda_0 GG \Lambda^{c-d} \text{ with } \Lambda_0 = \frac{\delta \Sigma^V}{\delta G}. \quad (24)$$

Not only in the BSE, but also for the expression for $\bar{\Sigma}^{SF}$ given in Eq. (10), the separation in direct and crossed contribution is crucial. Up to now only the normal-state Green's function appeared in the equations, because we neglected the feedback effects of SC to the magnetic fluctuations. However, in the expression for the self-energy [Eq. (10)] the normal and anomalous parts appear and double arrow lines,


(25)

are used to distinguish the different functions. Since in the anomalous terms no extra loops are created,

(26)

the crossed and direct contributions enter both with the same sign in the equation for the self-energy:

$$\bar{\Sigma}_F^{SF} := \iint \tau^z \begin{pmatrix} 0 & F \Lambda^{c+d} \\ F^\dagger \Lambda^{c+d} & 0 \end{pmatrix}. \quad (27)$$

For the normal contribution (diagonal component in Nambu space) the situation is a bit more complicated because the loop rule has to be taken into account: If a crossed contribution is inserted inside the self-energy form in Eq. (10), then a loop is created [Eq. (28)], leading to a minus sign, while the direct terms do not lead to any additional loop and no sign change. This can be seen in the following graph:

$$(28)$$
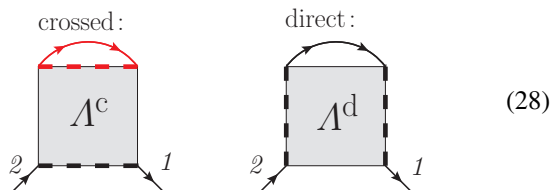
In the shorthand notation given in Eq. (10) this was not, strictly speaking, taken into account. The rigorous form of this equation instead reads

$$\bar{\Sigma}^{\text{SF}} := \iint d34\tau^z \begin{pmatrix} -G(3,4)\,\Lambda^{\text{c}-\text{d}}(1,3,2,4) & 0 \\ F^\dagger(3,4)\,\Lambda^{\text{c}+\text{d}}(3,1,2,4) & 0 \end{pmatrix}$$
$$+ \iint d34\tau^z \begin{pmatrix} 0 & F(3,4)\,\Lambda^{\text{c}+\text{d}}(1,3,4,2) \\ 0 & -G^\dagger(3,4)\,\Lambda^{\text{c}-\text{d}}(3,1,4,2) \end{pmatrix}.$$
$$(29)$$

Here it is shown explicitly how the direct contribution enters with different sign on the diagonal and off-diagonal Nambu component due to the loop rule. The way the four-point object is connected to the Green's function is shown in Eqs. (26) and (28) for the 21 and 22 elements of the self-energy. In the solution of the gap equation (see Sec. V), this sign difference will turn out to be crucial in order to have a nontrivial solution of the gap equation. Note that the self-energy derived from the Berk-Schrieffer interaction [53] satisfies the same sign convention as derived here.

Under the assumption of singlet SC pairing and magnetic collinearity, the normal part of the Green's function conserves spin, i.e., $G(1,2) = \delta_{\sigma_1\sigma_2} G_{\sigma_1}(\boldsymbol{r}_1,\tau_1,\boldsymbol{r}_2,\tau_2)$, while the anomalous part flips spin $F(1,2) = \delta_{\sigma_1-\sigma_2} F_{\sigma_1}(\boldsymbol{r}_1,\tau_1,\boldsymbol{r}_2,\tau_2)$. This aspect has no consequences for the $\bar{\Sigma}^{\text{GW}}$ and $\bar{\Sigma}^{\text{Ph}}$ parts of the self-energy Eqs. (1) and (2), since the interactions have no spin dependence. However, for the SF part in Eq. (29) the restriction leads to the result that

$$\bar{\Sigma}_{11} \text{ and } \bar{\Sigma}_{22} \quad \text{depend only on } \Lambda^{\text{c}-\text{d}}_{\sigma_1\sigma\sigma_2\sigma},$$

$$\bar{\Sigma}_{12} \text{ and } \bar{\Sigma}_{21} \quad \text{depend only on } \Lambda^{\text{c}+\text{d}}_{\sigma_1\sigma-\sigma\sigma_2}.$$

Furthermore, by comparing with Eq. (16) it is clear that Λ^{c} has no $(\sigma,\sigma,-\sigma,-\sigma)$ component, while Λ^{d} has no component in the channel $(\sigma,-\sigma,\sigma,-\sigma)$. Therefore, the following identities hold:

$$\Lambda^{\text{c}+\text{d}}_{\sigma\sigma-\sigma-\sigma} = \Lambda^{\text{d}}_{\sigma\sigma-\sigma-\sigma} = -\Lambda^{\text{c}-\text{d}}_{\sigma\sigma-\sigma-\sigma}, \tag{30}$$

$$\Lambda^{\text{c}+\text{d}}_{\sigma-\sigma\sigma-\sigma} = \Lambda^{\text{c}}_{\sigma-\sigma\sigma-\sigma} = \Lambda^{\text{c}-\text{d}}_{\sigma-\sigma\sigma-\sigma}. \tag{31}$$

These relations lead to a self-energy containing only $\Lambda^{\text{c-d}}$ and not $\Lambda^{\text{c}\pm\text{d}}$:

$$\bar{\Sigma}^{\text{SF}}_{11} = -\delta_{\sigma_1\sigma_2} G_{\sigma_1} \sum_\sigma \Lambda^{\text{c}-\text{d}}_{\sigma_1\sigma\sigma_1\sigma}, \tag{32}$$

$$\bar{\Sigma}^{\text{SF}}_{22} = \delta_{\sigma_1\sigma_2} G^\dagger_{\sigma_1} \sum_\sigma \Lambda^{\text{c}-\text{d}}_{\sigma\sigma_1\sigma\sigma_1}, \tag{33}$$

$$\bar{\Sigma}^{\text{SF}}_{12} = \delta_{\sigma_1-\sigma_2} F_{\sigma_1} \sum_\sigma \left(1 - 2\delta_{\sigma\sigma_1}\right) \Lambda^{\text{c}-\text{d}}_{\sigma_1\sigma-\sigma-\sigma_1}, \tag{34}$$

$$\bar{\Sigma}^{\text{SF}}_{21} = -\delta_{\sigma_1-\sigma_2} F^\dagger_{\sigma_1} \sum_\sigma \left(1 - 2\delta_{\sigma\sigma_1}\right) \Lambda^{\text{c}-\text{d}}_{\sigma\sigma_1-\sigma_1-\sigma}. \tag{35}$$

This is a convenient result, because we have to solve only one BSE for $\Lambda^{\text{c}-\text{d}}$ [Eq. (24)] and not the two separate equations for the direct and crossed parts. In the previous expression we use a concise notation in which the integrals are not written out [compare with Eq. (29)]. We use this notation in the next section when it does not lead to any ambiguity in the formulas. Unless stated otherwise, the coordinates are contracted analogous to a matrix product.

C. Local approximation

In the preceding sections we have constructed an approximate form of the electronic Nambu self-energy that we believe contains the relevant contributions to account for a SF mediated pairing. However, even this approximate form is too complex to be used directly in simulations on real materials. The dimensionality of the four-point object $\Lambda^{\text{c}-\text{d}}$ in Eqs. (32) to (35) and the resulting integrals are simply too complex to handle. What would make a significant simplification and bring the computational cost of the method to an affordable level would be a two-point form of the interaction; meaning an approximate form that can be written as

$$\bar{\Sigma}^{\text{SF}}(1,2)_{ab} \overset{!}{=} \bar{G}(1,2)_{ab}\, \bar{w}^{\text{SF}}(1,2)_{ab}, \tag{36}$$

where $\bar{w}^{\text{SF}}$ is to be understood as an effective interaction between electrons that accounts for the SF pairing and a,b is the index with respect to the Nambu matrix. Of course, such a form can be obtained by a formal inversion of the above equation,

$$\bar{w}^{\text{SF}}(1,2)_{ab} = \frac{\iint \begin{pmatrix} -G\Lambda^{\text{c}-\text{d}} & F\Lambda^{\text{c}+\text{d}} \\ -F^\dagger\Lambda^{\text{c}+\text{d}} & G^\dagger\Lambda^{\text{c}-\text{d}} \end{pmatrix}_{ab}}{\bar{G}(1,2)_{ab}},$$

but this is of no use in practice, because one would need the four-point object $\Lambda^{\text{c}\pm\text{d}}$ in the first place.

To obtain a two-point form we make use of an additional approximation, already common in the context of band-structure calculations [49,54,55], to use the KS potential as a local approximation for Σ^{V}, namely,

$$\Sigma^{\text{V}}(1,2) \approx \delta_{\tau_1\tau_2}\delta_{\boldsymbol{r}_1\boldsymbol{r}_2} v^{\text{xc}}_{\sigma_1\sigma_2}(\boldsymbol{r}_1\tau_1). \tag{37}$$

The functional derivative [Eq. (24)] leads to the xc kernel f^{xc}, which is a two-point function in space-time but still a four-point object in spin ($\mathbf{x}_1 = \{\mathbf{r}_1\tau_1\}$):

$$\frac{\delta v^{\text{xc}}_{\sigma_1\sigma_2}(\boldsymbol{x}_1)}{\delta G(3,4)} = \sum_{\sigma_5\sigma_6} \int d\boldsymbol{x}_5 \underbrace{\frac{\delta v^{\text{xc}}_{\sigma_1\sigma_2}(\boldsymbol{x}_1)}{\delta\rho_{\sigma_5\sigma_6}(\boldsymbol{x}_5)}}_{f^{\text{xc}}} \frac{\delta\rho_{\sigma_5\sigma_6}(\boldsymbol{x}_5)}{\delta G(3,4)}$$

$$= \iint d5d6\, f^{\text{xc}}_{\sigma_1\sigma_2\sigma_5\sigma_6}(\boldsymbol{x}_1\boldsymbol{x}_5) \frac{\delta G(5,6)}{\delta G(3,4)}\delta_{x_5x_6}$$

$$= f^{\text{xc}}_{\sigma_1\sigma_2\sigma_3\sigma_4}(\boldsymbol{x}_1\boldsymbol{x}_3)\delta_{x_3x_4}.$$

If Eq. (24) is solved with the xc kernel and the full G is approximated by the KS one, the well-known Dyson equation from linear response density functional theory appears [56],

$$
\begin{aligned}
\Lambda^{\text{c-d}} &= 4 f^{\text{xc}} + 16 f^{\text{xc}} \underbrace{G^{\text{KS}} G^{\text{KS}}}_{=\chi^{\text{KS}}} f^{\text{xc}} \\
&\quad + 64 f^{\text{xc}} G^{\text{KS}} G^{\text{KS}} f^{\text{xc}} G^{\text{KS}} G^{\text{KS}} f^{\text{xc}} + \cdots \\
&= 4 f^{\text{xc}} + 16 f^{\text{xc}} \frac{\chi^{\text{KS}}}{1 - f^{\text{xc}} \chi^{\text{KS}}} f^{\text{xc}},
\end{aligned}
$$

leading to the proper part of the response function $P_{\sigma_1 \sigma_1 \sigma_2 \sigma_2}$. Since the Green's function is diagonal with respect to spin, the longitudinal and transverse parts of the response decouple:

$$
\Lambda^{\text{c-d}}_{\sigma_1 \sigma_1 \sigma_2 \sigma_2} = 4 f^{\text{xc}}_{\sigma_1 \sigma_1 \sigma_2 \sigma_2} + 16 \sum_{\sigma_6 \sigma_7} f^{\text{xc}}_{\sigma_1 \sigma_1 \sigma_6 \sigma_6} P_{\sigma_6 \sigma_6 \sigma_7 \sigma_7} f^{\text{xc}}_{\sigma_7 \sigma_7 \sigma_2 \sigma_2},
$$

(38)

$$
\Lambda^{\text{c-d}}_{\sigma -\sigma \sigma -\sigma} = 4 f^{\text{xc}}_{\sigma -\sigma -\sigma \sigma} + 16 f^{\text{xc}}_{\sigma -\sigma -\sigma \sigma} P_{\sigma -\sigma -\sigma \sigma} f^{\text{xc}}_{\sigma -\sigma -\sigma \sigma}.
$$

(39)

The proper part P is related to the full response function χ via the Dyson equation:

$$
\chi_{\sigma_1 \sigma_2 \sigma_3 \sigma_4} = P_{\sigma_1 \sigma_2 \sigma_3 \sigma_4} + \delta_{\sigma_1 \sigma_2} \delta_{\sigma_3 \sigma_4} \sum_{\sigma \sigma'} P_{\sigma_1 \sigma_2 \sigma \sigma} v \chi_{\sigma' \sigma' \sigma_3 \sigma_4}.
$$

(40)

The response function $\chi_{\sigma_1 \sigma_2 \sigma_3 \sigma_4}$ in the spin basis determines the change in the spin-resolved charge density induced by external fields and is defined as

$$
\chi_{\sigma_1 \sigma_2 \sigma_3 \sigma_4} (\boldsymbol{r}_1, \tau_1, \boldsymbol{r}_2, \tau_2) := \frac{\delta \rho_{\sigma_1 \sigma_2} (\boldsymbol{r}_1, \tau_1)}{\delta \varphi^{\text{ext}}_{\sigma_3 \sigma_4} (\boldsymbol{r}_2, \tau_2)}.
$$

The equations for $\Lambda^{\text{c-d}}$ will become more transparent if we rewrite the response quantities on the right-hand side of Eqs. (38) and (39) in components of the Pauli matrix; i.e.,

$$
\chi_{ij} (\boldsymbol{r}_1, \tau_1, \boldsymbol{r}_2, \tau_2) := \frac{\delta \rho_i (\boldsymbol{r}_1, \tau_1)}{\delta \varphi^{\text{ext}}_j (\boldsymbol{r}_2, \tau_2)}.
$$

In this form χ represents the change of the electronic charge ρ or magnetic moment $\boldsymbol{m}$ ($\rho_i = \{\rho, m_x, m_y, m_z\}$) with respect to physical fields ($\varphi^{\text{ext}}_j = \{\varphi^{\text{ext}}_0, B^{\text{ext}}_x, B^{\text{ext}}_y, B^{\text{ext}}_z\}$). In this work we label the Pauli index with i and j and it should not be confused with the Nambu index indicated by a and b [used in Eq. (36)]. The basis transformations between the two representations are simply

$$
A_{\alpha \beta \gamma \delta} = \frac{1}{4} \sum_{ij} \sigma^i_{\alpha \beta} A_{ij} \sigma^j_{\gamma \delta},
$$

$$
A_{ij} = \sum_{\alpha \beta \gamma \delta} \sigma^i_{\beta \alpha} A_{\alpha \beta \gamma \delta} \sigma^j_{\delta \gamma},
$$

where σ^i is the four-component vector containing the Pauli matrices:

$$
\sigma^i = \left\{ \begin{pmatrix} 1 & 0 \\ 0 & 1 \end{pmatrix}, \begin{pmatrix} 0 & 1 \\ 1 & 0 \end{pmatrix}, \begin{pmatrix} 0 & -i \\ i & 0 \end{pmatrix}, \begin{pmatrix} 1 & 0 \\ 0 & -1 \end{pmatrix} \right\}.
$$

Note that the response function is a sparse matrix for the considered collinear system,

$$
\chi_{ij} = \begin{pmatrix} \chi_{xx} & \chi_{xy} & 0 & 0 \\ \chi_{yx} & \chi_{yy} & 0 & 0 \\ 0 & 0 & \chi_{zz} & \chi_{z0} \\ 0 & 0 & \chi_{0z} & \chi_{00} \end{pmatrix},
$$

and the proper and full responses are equal $\chi_{ij} = P_{ij}$ if $i, j \in \{x, y\}$ [Eq. (40)]. As mentioned above, we change the representation of the response function from spin to the Pauli basis in order to achieve a more transparent form of the effective interaction,

$$
\Lambda^{\text{c-d}}_{\sigma_1 \sigma_1 \sigma_2 \sigma_2} = \sum_{ij \in \{0,z\}} f^{\text{T}}_{i \sigma_1} P_{ij} (1 - \delta_{i0} \delta_{j0}) f_{j \sigma_2},
$$

(41)

$$
\Lambda^{\text{c-d}}_{\sigma -\sigma \sigma -\sigma} = 2 f^{\text{F}}_\sigma \chi^{\text{F}}_\sigma f^{\text{F}}_\sigma,
$$

(42)

where the two point functions $f_{i\sigma}$ and f^{F}_σ are given by ($z_\uparrow = +1, z_\downarrow = -1$)

$$
\begin{aligned}
f^{\text{T}}_{z\sigma} &:= z_\sigma f^{\text{xc}}_{zz} + f^{\text{xc}}_{0z} & f_{z\sigma} &:= z_\sigma f^{\text{xc}}_{zz} + f^{\text{xc}}_{z0}, \\
f^{\text{T}}_{0\sigma} &:= f^{\text{xc}}_{00} + z_\sigma f^{\text{xc}}_{z0} & f_{0\sigma} &:= f^{\text{xc}}_{00} + z_\sigma f^{\text{xc}}_{0z}, \\
f^{\text{F}}_\sigma &:= f^{\text{xc}}_{xx} + z_\sigma i f^{\text{xc}}_{xy} & \chi^{\text{F}}_\sigma &:= \chi_{xx} + z_\sigma i \chi_{xy}.
\end{aligned}
$$

In Eq. (41) we have dropped $f^{\text{xc}}_{\sigma_1 \sigma_1 \sigma_2 \sigma_2} + f^{\text{T}}_{0\sigma_1} P_{00} f_{0\sigma_2}$ in order to avoid any double counting: This term is, in fact, already accounted for by the screened Coulomb interaction w in the GW term, which contains an analogous contribution in the form $v + v P_{00} v + \cdots$. In addition, we neglect the linear order $f^{\text{xc}}_{\sigma -\sigma -\sigma \sigma}$, because in a system featuring magnetic fluctuations it is supposed to be small as compared to the dominant $f^{\text{F}}_\sigma \chi^{\text{F}}_\sigma f^{\text{F}}_\sigma$ term. This is because the SFs should appear as a large value of the magnetic susceptibility.

The form of $\Lambda^{\text{c-d}}$ in Eq. (42) has now obtained an immediate physical interpretation: The exchange-correlation kernels f^{xc} act as a vertex for the electronic interaction mediated by SFs, which are expressed by the magnetic susceptibility χ.

The transverse part allows for a flip of the electronic spin, which can be understood in the following way.

(1) The spin flip of electron 1 corresponds to a local fluctuation in the magnetic moment δm_1.

(2) This, in turn, creates a magnetic field via the kernel: $\delta B_1 = f^{\text{xc}} \delta m_1$.

(3) If the system features magnetic fluctuations, the δB_1 leads to fluctuations in the system: $\delta m_2 = \chi \delta B_1$.

(4) The fluctuation (magnons) couple via the second kernel to another electron $\delta B_2 = f^{\text{xc}} \delta m_2$, whose spin is flipped in the absorption process.

This interpretation is analogous to the one given by Kukkonen and Overhauser for the charge fluctuations [29] and shows that the term $\Lambda^{\text{c-d}}$ in the local form represents an effective interaction between electrons mediated by magnetic fluctuations.

The final $\bar{\Sigma}^{\text{SF}}$ is constructed by inserting the two-point particle-hole propagators given in Eqs. (41) and (42) in the equation for the self-energy Eqs. (32) to (35). We do this in the next section. Note that by doing so, a separation in direct and

crossed contribution is implied for the xc kernel [see Eqs. (30) and (31)]. This is an assumption because the xc kernel is, in general, not based on a diagrammatic expansion.

IV. FINAL FORM OF THE SELF-ENERGY

So far our formalism has been derived for collinear magnetic systems and therefore it could be applied to general interactions between SC and magnetism. In its nonsuperconducting limit our effective interaction is very similar to that Schweflinghaus *et al.* [57] used to investigate the effect of magnetic ions on a metallic substrate. We now simplify it for the case of a nonmagnetic system. This means that, by construction, we do not consider the possibility of atomic scale coexistence between magnetism and SC. We believe that this assumption is justified for a large set of hi-T_c SC (cuprates and pnictides), where usually (although exceptions have been observed) the antiferromagnetic (AFM) order is completely suppressed in the SC regime [8,58].

In a nonmagnetic system the response functions and xc kernel are diagonal with respect to the Pauli index and the three directions with respect to the magnetic field are degenerate. In this case the effective interaction in Eqs. (41) and (42) reduces to a simple form (here $\boldsymbol{x}$ is a combined variable of space and time $\boldsymbol{x} = \{\boldsymbol{r}\tau\}$):

$$\Lambda^{\text{c-d}}_{\sigma_1\sigma_1\sigma_2\sigma_2}(\boldsymbol{x}_1,\boldsymbol{x}_2) = z_{\sigma_1} z_{\sigma_2} \frac{1}{2} \Lambda^{\text{SF}}(\boldsymbol{x}_1,\boldsymbol{x}_2),$$

$$\Lambda^{\text{c-d}}_{\sigma-\sigma\sigma-\sigma}(\boldsymbol{x}_1,\boldsymbol{x}_2) = \Lambda^{\text{SF}}(\boldsymbol{x}_1,\boldsymbol{x}_2),$$

$$\Lambda^{\text{SF}}(\boldsymbol{x}_1,\boldsymbol{x}_2) := 2 \iint d\boldsymbol{x} d\boldsymbol{x}'$$
$$\times f^{\text{xc}}_{zz}(\boldsymbol{x}_1,\boldsymbol{x}) \chi_{zz}(\boldsymbol{x}\boldsymbol{x}') f^{\text{xc}}_{zz}(\boldsymbol{x}',\boldsymbol{x}_2), \quad (43)$$

and we insert this form in Eqs. (32) to (35):

$$\bar{\Sigma}^{\text{SF}}_{ab}(\boldsymbol{x}_1,\boldsymbol{x}_2) = \frac{3}{2}(-1)^{b+1} \Lambda^{\text{SF}}(\boldsymbol{x}_1,\boldsymbol{x}_2) \bar{G}_{ab}(\boldsymbol{x}_1,\boldsymbol{x}_2). \quad (44)$$

The prefactor represents the fact that the diagonal part enters with the opposite sign due to the effect of the loop rule discussed in Sec. III B. By construction, the equation has the GW form, however with an interaction originating from SF and denoted as Λ^{SF}. Note that this effective interaction, in the limit of an homogeneous electron gas, reduces to the form derived by Vignale and Singwi in Ref. [50]. Λ^{SF} contains the xc kernel and the magnetic response function, which can be calculated using Time-Dependent DFT (TD-DFT) [56]. The total self-energy is given by the sum of $\bar{\Sigma}^{\text{GW}}$, $\bar{\Sigma}^{\text{SF}}$, and $\bar{\Sigma}^{\text{Ph}}$ given in Eqs. (1), (44), and (2), respectively.

Relation to previous approaches

So far, the challenge to describe unconventional SC has been taken up by model methods. Among the most successful approaches for iron pnictides is to map the systems on a multi-band Hubbard model and to seek the solution of this model. Common methods for this are the functional renormalization group [59], used, for example, by Platt, Thomale, and Hanke [60], the fluctuation exchange approximation [61], as adopted by Kuroki and co-workers [62] or Graser and co-workers [63], or a Berk and Schrieffer [53] interaction, as discussed in Ref. [64].

In this respect is important to notice that our effective interaction [Eq. (43)] is formally similar to that of Berk and Schrieffer. However, since we construct it from the exact TD-DFT susceptibility and the exchange-correlation kernel f_{xc}, it neither requires the mapping on a Hubbard Hamiltonian, nor the use of any parameter as the U.

V. THE FUNCTIONAL

So far, we have derived the contribution from the SFs to the self-energy and, correspondingly, a SF pairing that can be used in any theory of SC. In this section we specialize this result to be used within the framework of SCDFT. To do this we make use of the Sham-Schlüter connection [65] between a KS and an interacting system, generalized to the SC case by Marques [66]. We assume that v^{xc} and the diagonal part of $\bar{\Sigma}^{\text{GW}}$ act in a similar way as a mass operator on the Hartree states and cancel each other. Then the noninteracting SC-KS is mapped to the interacting system by the following self-energy form:

$$\bar{\Sigma}^{\text{SS}} = \bar{\Sigma}^{\text{GW}} + \bar{\Sigma}^{\text{SF}} + \bar{\Sigma}^{\text{Ph}} - \begin{pmatrix} \text{GW} & \Delta^{\text{xc}*} \\ \Delta^{\text{xc}} & -G^{\dagger}w \end{pmatrix}. \quad (45)$$

The Sham-Schlüter connection follows by imposing that the total density $\rho(\boldsymbol{r}_1) = \lim_{\boldsymbol{r}_1 \to \boldsymbol{r}_2} \frac{2}{\beta} \sum_{\omega_n} G(\boldsymbol{r}_1,\boldsymbol{r}_2,\omega_n)$ and the anomalous density $\chi(\boldsymbol{r}_1,\boldsymbol{r}_2) = \sum_{\omega_n} F(\boldsymbol{r}_1,\boldsymbol{r}_2,\omega_n)$ are identical in the KS and interacting system:

$$0 = \delta_{ab} \lim_{\boldsymbol{r}_1 \to \boldsymbol{r}_2} \frac{2}{\beta} \sum_{\omega_n} e^{i\omega_n 0^+} [\bar{G}^{\text{KS}} \bar{\Sigma}^{\text{SS}} \bar{G}]_{ab},$$

$$0 = (1 - \delta_{ab}) \frac{1}{\beta} \sum_{\omega_n} e^{i\omega_n 0^+} [\bar{G}^{\text{KS}} \bar{\Sigma}^{\text{SS}} \bar{G}]_{ab}.$$

The connection becomes a closed equation for the superconducting gap by approximating the full Green's function on the right-hand side and the one in $\bar{\Sigma}$ with the KS one. In addition, we neglect all contributions that are explicitly higher than linear in the pairing potential. Since, as discussed in Sec. III, we are mostly concerned with computing an accurate critical temperature, rather than the full temperature dependence of the superconducting gap. In this approximation, the 12 element of the Sham-Schlüter equation simplifies to

$$0 = \frac{1}{\beta} \sum_n e^{i\omega_n 0^+} G^{\text{KS}} G^{\text{KS}\dagger} \Delta^{\text{xc}*}$$
$$+ \frac{1}{\beta} \sum_n e^{i\omega_n 0^+} G^{\text{KS}} \bar{\Sigma}_{11} F^{\text{KS}}$$
$$- \frac{1}{\beta} \sum_n e^{i\omega_n 0^+} G^{\text{KS}} \bar{\Sigma}_{12} G^{\text{KS}\dagger}.$$

The Matsubara summation may be evaluated analytically because the frequency dependence of the KS Green's function is known and for the response functions and phonons a frequency representation with respect to the anti-Hermitian part of the retarded quantities holds [Eq. (5)]. The evaluation is done with the help of the residue theorem, which, for the

Matsubara summation of an analytic function $A(z)$, leads to

$$\frac{1}{\beta} \sum_n^\infty A(i\omega_n) = \sum_m^{\text{Poles} \in \gamma} \text{res}[f_\beta(z)A(z), z_m], \qquad (46)$$

where the contour γ are two infinite half-circle excluding the imaginary axis and f_β is the Fermi distribution function. At this point an adiabatic approximation for the xc kernel is assumed. This reduces the order of poles in Λ^{SF} and the same residue are found for the Coulomb, phonon, and SF contribution. After the evaluation of the Matsubara sum [10], the equation is inverted for Δ_k^{xc}, leading to a gap equation very similar to the conventional one in Eq. (7):

$$\Delta_k^{\text{xc}} = -\Delta_k^{\text{xc}} \mathcal{Z}_k^D - \sum_{k'} \mathcal{K}_{kk'}^C \frac{\tanh\left(\frac{\beta E_{k'}}{2}\right)}{2E_{k'}} \Delta_{k'}^{\text{xc}},$$

$$\mathcal{Z}_k^D = \frac{1}{\pi} \sum_{k'} \int_0^\infty d\omega \frac{\text{Im}\left[\frac{3}{2}\Lambda_{kk'}^{\text{SF}}(\omega)\right] - \Lambda_{kk'}^{\text{Ph}}(\omega)}{2\tanh\left(\frac{\beta \zeta_k}{2}\right)} \frac{d}{d\zeta_k}$$

$$\times J^+(\zeta_k, \zeta_{k'}\omega),$$

$$\mathcal{K}_{kk'}^C = \frac{2}{\pi} \int_0^\infty d\omega \frac{\text{Im}\left[w_{kk'}(\omega) + \frac{3}{2}\Lambda_{kk'}^{\text{SF}}(\omega)\right] + \Lambda_{kk'}^{\text{Ph}}(\omega)}{\tanh\left(\frac{\beta \zeta_k}{2}\right)\tanh\left(\frac{\beta \zeta_{k'}}{2}\right)}$$

$$\times J^-(\zeta_k, \zeta_{k'}\omega),$$

$$I_\beta(\zeta, \zeta', \omega) := -f_\beta(\zeta)f_\beta(\zeta')b_\beta(\omega)$$

$$\times \left[\frac{e^{\beta\zeta} - e^{\beta(\zeta'+\omega)}}{\zeta - \zeta' - \omega} - \frac{e^{\beta\zeta'} - e^{\beta(\zeta+\omega)}}{\zeta - \zeta' + \omega}\right],$$

$$J_\beta^\pm(\zeta, \zeta', \omega) := I_\beta(\zeta, \zeta', \omega) \pm I_\beta(\zeta, -\zeta', \omega). \qquad (47)$$

$b_\beta(\omega)$ is the Bose distribution function and ζ_k are the single-particle KS energies of the non-SC system relative to the chemical potential $\zeta_k = \epsilon_k - \mu$. The kernels in this integral equation represent different physical processes introduced by the corresponding self-energy contribution.

(1) The $\Lambda_{kk'}^{\text{Ph}}(\omega)$ term describes pairing between electrons due to phonons. The interaction is attractive: $\Lambda_{kk'}^{\text{Ph}}(\omega) < 0$.

(2) The $w_{kk'}(\omega)$ term is the scattering of electrons due to Coulomb interaction. The bare Coulomb interaction is reduced by intermediate scattering processes (screening) $w = v\epsilon^{-1}$ [Eq. (4)]. Plasmonic effects may also enter via this term.

(3) The last term $\Lambda_{kk'}^{\text{SF}}(\omega)$ contains the magnetic response function χ_{zz} and hence becomes important if the system is close to a transition to a magnetic phase. In such a case the response function features sharp excitations, which represent paramagnons.

The two last terms originate both from the Coulomb interaction and are therefore intrinsically repulsive:

$$\text{Im}\left[\Lambda_{kk'}^{\text{SF}}(\omega)\right] > 0 \text{ and } \text{Im}\left[w_{kk'}(\omega)\right] > 0. \qquad (48)$$

If these are the strongest terms in the gap equation (47), in order to have a nontrivial solution, a sign change must occur in the gap function. We show how this mechanism works in the following section where we apply the formalism to

a model system and investigate the general structure of the theory.

VI. APPLICATION TO A TWO-BAND MODEL SYSTEM

A. Isotropic approximation and the two-band model with a SF pairing

The function Δ_{nk} is known to have a strong dependence on the ϵ_{nk}[18]. The remaining $\boldsymbol{k}$-space structure, however, is often of little importance, especially within topologically connected Fermi surface portions [15]. Therefore, it is convenient to define an isotropic (or multi-band-isotropic) approximation by means of the averaging operation

$$\Delta_{nk} \approx \Delta_n(E) := \frac{1}{N_n(E)} \sum_k \delta(\epsilon_{nk} - E)\Delta_{nk},$$

$$N_n(E) := \sum_k \delta(\epsilon_{nk} - E),$$

where $N_n(E)$ is the density of states of band n. This simplification leads to an isotropic gap equation, where all interactions are replaced with energy- and band-dependent quantities. As an example of how this averaging works, we consider the SF term:

$$\Lambda_{nn'}^{\text{SF}}(E, E', \omega) \approx \frac{1}{N_n(E)} \sum_{kk'} \Lambda_{nkn'k'}^{\text{SF}}(\omega)$$

$$\times \delta(\epsilon_{nk} - E)\delta(\epsilon_{n'k'} - E').$$

We assume the system to be close to an AFM instability with the ordering and nesting vector $\boldsymbol{q}_c$. Then the proximity to the magnetic phase leads to strong fluctuations (paramagnons) at low frequencies and the vector $\boldsymbol{q}_c$ in the magnetic response function $\chi_{zz}(\omega, \boldsymbol{q})$ [67]. These fluctuations are expected to be weak for other vectors. The portions (bands) of the Fermi surface nested by $\boldsymbol{q}_c$ are labeled as $n = +$ and $n = -$.

The usual TD-DFT kernels like the adiabatic local density approximation have no dependence on $(\omega, \boldsymbol{q})$ and the form of Λ^{SF} in frequency and $\boldsymbol{q}$ is determined by χ_{zz}.

In such a situation the isotropic effective interaction is expected to be small for intraband scattering ($\Lambda_{\pm\pm}^{\text{SF}} \approx 0$) and peaked for interband scattering ($\Lambda_{\pm\mp}^{\text{SF}}$).

This situation is modeled by a simple parabola centered around a characteristic frequency $\bar{\omega}$ (see Fig. 2, top right; we have also tested a Gaussian and a Lorentzian form and we find that the shape has little effect on the properties of the model):

$$\Lambda_{IJ}^{\text{SF}}(E, E', \omega) = \begin{cases} c_1 N_J(E')\left[1 - \left(\frac{\omega - \bar{\omega} - \frac{c_2}{2}}{c_2}\right)^2\right], \\ \text{if } |\omega - \bar{\omega}| \leqslant \frac{c_2}{2} \text{ and } I \neq J, \\ 0 \text{ elsewhere.} \end{cases} \qquad (49)$$

We fix the width c_2 to a value of 0.01 Ry and the density of states times the peak height c_1 is determined by requiring a value for the effective coupling strength λ^{SF}. The effective coupling strength is given by the integral of Λ_{IJ}^{SF} with respect to ω:

$$\lambda_{IJ}^{\text{SF}} := \frac{3}{2\pi} \int_0^\infty d\omega \frac{2\Lambda_{IJ}^{\text{SF}}(\epsilon_F, \epsilon_F, \omega)}{\omega}.$$
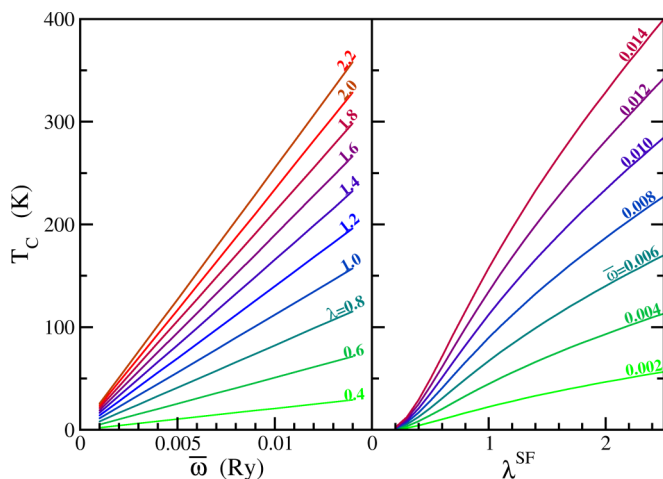
FIG. 1. (Color online) (Left) T_c for different λ^{SF} as a function of the average $\bar{\omega}$. (Right) Analogous plot, here for several $\bar{\omega}$ as a function of λ^{SF}.

Within this simple multiband isotropic model the structure of our SF theory of SC can be made more transparent.

B. Discussion of the SF contribution

Here and in the next section, we assume a two-band isotropic approximation discussed in the previous section. In this way we try to investigate the general solution of the SCDFT gap equation for a SF-mediated pairing. As a first step we neglect completely Coulomb and phonon contributions, considering only the SF interaction given in Eq. (49).

We modify the SF by acting on the parameters $\bar{\omega}$ and λ_{IJ}^{SF}. In Fig. 1 we show the critical temperature as a function of $\bar{\omega}$ and λ_{IJ}^{SF}. From Eliashberg theory for phonon-driven superconductors we have knowledge of the following relations between characteristic frequency and average coupling strength [68,69]:

$$T_c \propto \bar{\omega}\, e^{-\alpha/\lambda} \quad \text{for small } \lambda, \tag{50}$$

$$T_c \propto \bar{\omega}\, \sqrt{\lambda} \quad \text{for large } \lambda. \tag{51}$$

On the right-hand side of Fig. 1 we can recognize the exponential and square-root behavior with respect to λ^{SF}. The transition between small and large coupling takes place at $\lambda^{SF} \sim 1.5$ for $\bar{\omega} = 0.15$ Ry. For the dependence of T_c with respect to $\bar{\omega}$, we find a linear behavior.

This result is not accidental, because the sign change of the gap leads effectively to an attractive interaction between the two bands; therefore, within this simplified model there is no formal difference between SF repulsive pairing and conventional phononic attraction.

Within such a model calculation we can estimate the coupling strength in the iron-based superconductors, simply by the experimental knowledge that the characteristic energy of the magnetic fluctuations are of about 20 meV [5]. This implies a coupling λ^{SF} of about 1 (neglecting phononic and Coulomb effects) to reach the critical temperatures of ~ 10 K found in these compounds.
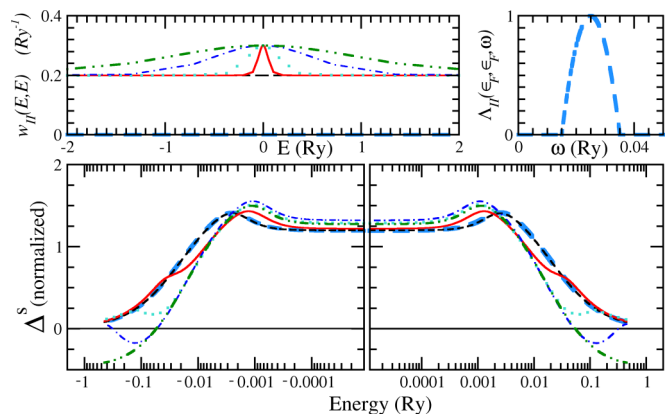

FIG. 2. (Color online) (Top left) Form of the Coulomb interaction for various κ determining the decay of the Coulomb interaction [Eq. (52)]. (Top right) Form of the SF interaction Eq. (49). (Bottom) Gap function Δ_+ as a function of energy and κ.

C. Interplay between Coulomb, spin-fluctuation, and phonon contribution

In the previous section we have observed that the features of the SCDFT gap equation with a SF interaction is relatively simple and similar to the conventional phononic case. Here we add the effect of phonon and Coulomb interactions. This will create a frustration on the SC potential because the three interaction will compete against each other.

We use the same SF spectrum in Eq. (49) and fix $\lambda^{SF} = 1.2$ and $\bar{\omega} = 0.01$ Ry. The Coulomb interaction is very different in nature, compared to the SF. In particular, its frequency dependence develops in the plasmonic energy scale (eV). We therefore ignore it and assume a flat interaction with respect to ω.

It is expected that this interaction decays like $\frac{1}{q^2 + q_{TF}^2}$, where q_{TF} is the Thomas-Fermi screening vector. Therefore, the contribution for small momentum transfer (intraband) should be much larger than the interband contribution corresponding to $q_c \approx k - k'$. Similarly for scattering from the Fermi level to high-energy states, the scattering should become momentum independent [70]. We model this picture in the following way:

$$w_{IJ}(E_1, E_2) = \begin{cases} N_J(E_2)\big(U_0 + U_1 e^{-\kappa(E_1^2 + E_2^2)}\big) \\ \quad \text{if} \quad I = J, \\ N_J(E_2)U_0 \\ \quad \text{if} \quad I \neq J. \end{cases} \tag{52}$$

The diagonal part $w_{II}(E_1, E_1)$ of this interaction is shown in Fig. 2. For the parameters of the Coulomb interaction we choose $N_J(\epsilon_F)U_0 = 0.2, U_1 = \frac{U_0}{2}$. The parameter κ is used to control the Coulomb interaction: If κ is large the Coulomb interaction decays very quickly in energy.

Due to the choice of an electron hole symmetric DOS [$N_+(E) = N_-(E)$] and interaction, the gap function is also totally symmetric: $\Delta_I(E) = \Delta_I(-E)$ and $\Delta_+(E) = -\Delta_-(E)$ and hence only the positive branch $\Delta_+(E)$ is shown in Fig. 2. Note that within this symmetry a constant Coulomb interaction ($\kappa \to \infty$) cancels out completely from the gap equation (47).

In general, the gap function shows a typical form, being constant close to the Fermi level, followed by an extremum and a decay for larger energies [18,71]. By decreasing the value
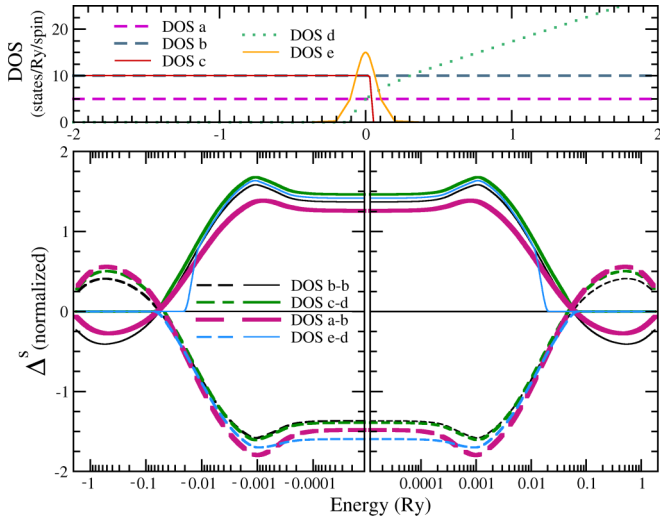
FIG. 3. (Color online) Gap $\Delta_{\pm}$ for different asymmetric density of states.

of κ the Coulomb contribution starts to influence the results. The critical temperature decreases, due to repulsion within one band, and the gap starts to show dips. The dips indicate the regime, where the Coulomb interaction competes with the SF. For $\kappa < 1$ the Coulomb contributions are strong enough to flip the sign of the gap function for certain energies. The sign change of the gap function at higher energies reduces the effect related to the repulsive Coulomb term in the gap equation (47).

Effectively, the Coulomb contribution on the full energy scale may be mapped to a reduced effective Coulomb term on a smaller energy scale due to the sign change of the gap function. Hence, the sign change of the gap function is the way Coulomb renormalization happens in SCDFT [18,70]. Note that the sign change of the gap happens far away from the Fermi level.

However, for $\kappa = 4$ the Coulomb contribution still decays faster in energy than the SF term, which leads to one more sign change in the large energy regime (dash-dotted blue line in Fig. 2). If we decrease the κ further, the Coulomb contributions dominate also in the large energy range and the gap changes sign only once.

Note that the critical temperature converges quickly with respect to κ. This indicates that the Coulomb interaction influences the critical temperature only in a small energy window for the symmetric two-band system and the renormalization of the gap is not affecting the critical temperature strongly.

To verify this observation, we test different densities of states instead of the constant one used so far: The different

functions are step and square-root functions, which represent a two- and three-dimensional system, respectively, and a Gaussian peak. The different functions are shown in Fig. 3. The non-flat functions cut away the long energy tails of the gap function. However, the effect on the critical temperature is rather small.

What has a strong effect on T_c is a change of the ratio $\frac{N_+(\epsilon_F)}{N_-(\epsilon_F)} = 1$ (magenta line in Fig. 2). This verifies that in the two-band system with a sign-changing gap, only a small energy region around the Fermi level matters for the Coulomb repulsion. This is very different from the one-band case, where the Coulomb renormalization at large energies is an essential effect.

Last, we consider the inclusion of the purely attractive phonon contribution. Its behavior is rather straightforward. If a single phonon peak is included [Eq. (49)] providing the same coupling between all bands, the critical temperature reduces by increasing λ^{Ph}. Until a the phononic coupling strength reaches the value of λ^{SF}. The phonons dominate the gap equation and the symmetry of the gap changes. The $s_{\pm}$ state favored by the repulsive interactions is suppressed and an s_{++} state is found. From this point the T_c starts to rise again with increasing λ^{Ph}.

VII. SUMMARY AND OUTLOOK

In this work we have derived a fully *ab initio* effective electron-electron interaction containing the effect of a pairing mediated by SF. The derivation starts from many-body perturbation theory and the introduction of a self-energy function, containing the relevant diagrams originating from its vertex part, therefore going beyond the GW approximation. The vertex correction enter the expression in the form of the particle-hole propagator, which is a highly nonlocal object determined by a BSE. The solution of the BSE would be computationally not feasible for realistic systems instead; in Sec. III C, we propose a local approximation for the particle-hole propagator. In this limit the equation for the self-energy becomes very transparent: SFs enter via the magnetic response functions, which can be calculated effectively [67,72] within linear response TD-DFT, and the coupling to the electrons is mediated by the exchange-correlation kernel.

This effective interaction is, in principle, applicable to any theory of SC; however, in this work we cast it into the framework of SCDFT by the construction of an explicit xc kernel (Sec. V). In this way the full gap equation remains completely parameter free.

We show a first application of the new functional (Sec. VI) to a two-band electron gas model. Application to real materials will follow; however, this further step needs the calculation of the magnetic response function for the real system and will be the subject to further investigation.

[1] J. Bednorz and K. Müller, Z. Phys. B: Condens. Matter **64**, 189 (1986).

[2] J. G. Bednorz and K. A. Müller, Rev. Mod. Phys. **60**, 585 (1988).

[3] Y. Kamihara, H. Hiramatsu, M. Hirano, R. Kawamura, H. Yanagi, T. Kamiya, and H. Hosono, J. Am. Chem. Soc. **128**, 10012 (2006).

[4] P. Hirschfeld, M. Korshunov, and I. Mazin, Rep. Prog. Phys. **74**, 124508 (2011).

[5] G. R. Stewart, Rev. Mod. Phys. **83**, 1589 (2011).

[6] D. Manske, *Theory of Unconventional Superconductors, Cooper-Pairing Mediated by Spin Excitations* (Springer-Verlag, Berlin, Heidelberg, 2004).

[7] T. Saito, S. Onari, and H. Kontani, Phys. Rev. B **82**, 144510 (2010).

[8] P. A. Lee, N. Nagaosa, and X.-G. Wen, Rev. Mod. Phys. **78**, 17 (2006).

[9] L. N. Oliveira, E. K. U. Gross, and W. Kohn, Phys. Rev. Lett. **60**, 2430 (1988).

[10] M. Lüders, M. A. L. Marques, N. N. Lathiotakis, A. Floris, G. Profeta, L. Fast, A. Continenza, S. Massidda, and E. K. U. Gross, Phys. Rev. B **72**, 024545 (2005).

[11] A. Sanna and E. K. U. Gross (unpublished).

[12] A. Floris, G. Profeta, N. N. Lathiotakis, M. Lüders, M. A. L. Marques, C. Franchini, E. K. U. Gross, A. Continenza, and S. Massidda, Phys. Rev. Lett. **94**, 037004 (2005).

[13] G. Profeta, C. Franchini, N. N. Lathiotakis, A. Floris, A. Sanna, M. A. L. Marques, M. Lüders, S. Massidda, E. K. U. Gross, and A. Continenza, Phys. Rev. Lett. **96**, 047003 (2006).

[14] A. Sanna, G. Profeta, A. Floris, A. Marini, E. K. U. Gross, and S. Massidda, Phys. Rev. B **75**, 020511 (2007).

[15] A. Floris, A. Sanna, S. Massidda, and E. K. U. Gross, Phys. Rev. B **75**, 054508 (2007).

[16] P. Cudazzo, G. Profeta, A. Sanna, A. Floris, A. Continenza, S. Massidda, and E. K. U. Gross, Phys. Rev. Lett. **100**, 257001 (2008).

[17] P. Cudazzo, G. Profeta, A. Sanna, A. Floris, A. Continenza, S. Massidda, and E. K. U. Gross, Phys. Rev. B **81**, 134506 (2010).

[18] M. A. L. Marques, M. Lüders, N. N. Lathiotakis, G. Profeta, A. Floris, L. Fast, A. Continenza, E. K. U. Gross, and S. Massidda, Phys. Rev. B **72**, 024546 (2005).

[19] R. Akashi and R. Arita, Phys. Rev. Lett. **111**, 057006 (2013).

[20] C. Bersier, A. Floris, A. Sanna, G. Profeta, A. Continenza, E. K. U. Gross, and S. Massidda, Phys. Rev. B **79**, 104503 (2009).

[21] A. Sanna, C. Franchini, A. Floris, G. Profeta, N. N. Lathiotakis, M. Lüders, M. A. L. Marques, E. K. U. Gross, A. Continenza, and S. Massidda, Phys. Rev. B **73**, 144512 (2006).

[22] L. Boeri, O. V. Dolgov, and A. A. Golubov, Phys. Rev. Lett. **101**, 026403 (2008).

[23] P. Morel and P. W. Anderson, Phys. Rev. **125**, 1263 (1962).

[24] I. I. Mazin, D. J. Singh, M. D. Johannes, and M. H. Du, Phys. Rev. Lett. **101**, 057003 (2008).

[25] O. V. Dolgov, I. I. Mazin, A. A. Golubov, S. Y. Savrasov, and E. G. Maksimov, Phys. Rev. Lett. **95**, 257003 (2005).

[26] P. Hohenberg and W. Kohn, Phys. Rev. **136**, B864 (1964).

[27] T. Kreibich, R. van Leeuwen, and E. K. U. Gross, Phys. Rev. A **78**, 022501 (2008).

[28] Y. Nambu, Phys. Rev. **117**, 648 (1960).

[29] C. A. Kukkonen and A. W. Overhauser, Phys. Rev. B **20**, 550 (1979).

[30] E. K. U. Gross and S. Kurth, Int. J. Quantum Chem. **40**, 289 (1991).

[31] J. Bardeen, L. N. Cooper, and J. R. Schrieffer, Phys. Rev. **108**, 1175 (1957).

[32] R. S. Gonnelli, D. Daghero, D. Delaude, M. Tortello, G. A. Ummarino, V. A. Stepanov, J. S. Kim, R. K. Kremer, A. Sanna, G. Profeta, and S. Massidda, Phys. Rev. Lett. **100**, 207004 (2008).

[33] C. Bersier, A. Floris, P. Cudazzo, G. Profeta, A. Sanna, F. Bernardini, M. Monni, S. Pittalis, S. Sharma, H. Glawe, A. Continenza, S. Massidda, and E. K. U. Gross, J. Phys.: Condens. Matter **21**, 164209 (2009).

[34] C. C. Tsuei and J. R. Kirtley, Rev. Mod. Phys. **72**, 969 (2000).

[35] L. Hedin, Phys. Rev. **139**, A796 (1965).

[36] A. B. Migdal, J. Exptl. Theoret. Phys. **34**, 1438 (1958) [Sov. Phys. JETP **34**, 996 (1958)].

[37] T. A. Maier, S. Graser, D. J. Scalapino, and P. Hirschfeld, Phys. Rev. B **79**, 134520 (2009).

[38] J. Wen, G. Xu, Z. Xu, Z. W. Lin, Q. Li, Y. Chen, S. Chi, G. Gu, and J. M. Tranquada, Phys. Rev. B **81**, 100513 (2010).

[39] S. M. Shapiro, G. Shirane, and J. D. Axe, Phys. Rev. B **12**, 4899 (1975).

[40] R. E. Prange, Phys. Rev. **129**, 2495 (1963).

[41] A more general and unbiased way would be to start from Hedin cycle [35] and iterate it self-consistently. This would lead also include the T-matrix diagrams considered here, but at a slow convergence rate [35].

[42] G. Baym and L. P. Kadanoff, Phys. Rev. **124**, 287 (1961).

[43] E. Sasioglu, A. Schindlmayr, C. Friedrich, F. Freimuth, and S. Blügel, Phys. Rev. B **81**, 054434 (2010).

[44] G. Onida, L. Reining, and A. Rubio, Rev. Mod. Phys. **74**, 601 (2002).

[45] E. E. Salpeter and H. A. Bethe, Phys. Rev. **84**, 1232 (1951).

[46] J. Hertz and D. Edwards, J. Phys. F: Met. Phys. **3**, 2174 (1973).

[47] S. Doniach and S. Engelsberg, Phys. Rev. Lett. **17**, 750 (1966).

[48] V. P. Zhukov, E. V. Chulkov, and P. M. Echenique, Phys. Rev. B **72**, 155109 (2005).

[49] P. Romaniello, F. Bechstedt, and L. Reining, Phys. Rev. B **85**, 155131 (2012).

[50] G. Vignale and K. S. Singwi, Phys. Rev. B **32**, 2156 (1985).

[51] L. G. Molinari, Phys. Rev. B **71**, 113102 (2005).

[52] F. Aryasetiawan and S. Biermann, Phys. Rev. Lett. **100**, 116402 (2008).

[53] N. F. Berk and J. R. Schrieffer, Phys. Rev. Lett. **17**, 433 (1966).

[54] L. J. Sham and W. Kohn, Phys. Rev. **145**, 561 (1966).

[55] R. Del Sole, L. Reining, and R. W. Godby, Phys. Rev. B **49**, 8024 (1994).

[56] E. Runge and E. K. U. Gross, Phys. Rev. Lett. **52**, 997 (1984).

[57] B. Schweflinghaus, M. dos Santos Dias, A. T. Costa, and S. Lounis, Phys. Rev. B **89**, 235439 (2014).

[58] I. Mazin, Nature (London) **464**, 183 (2010).

[59] R. Shankar, Rev. Mod. Phys. **66**, 129 (1994).

[60] C. Platt, R. Thomale, and W. Hanke, Phys. Rev. B **84**, 235121 (2011).

[61] N. Bickers and D. Scalapino, Ann. Phys. **193**, 206 (1989).

[62] K. Kuroki, S. Onari, R. Arita, H. Usui, Y. Tanaka, H. Kontani, and H. Aoki, Phys. Rev. Lett. **101**, 087004 (2008).

[63] S. Graser, T. A. Maier, P. J. Hirschfeld, and D. J. Scalapino, New J. Phys. **11**, 025016 (2009).

[64] P. J. Hirschfeld, M. M. Korshunov, and I. I. Mazin, Rep. Prog. Phys. **74**, 124508 (2011).

[65] L. J. Sham and M. Schlüter, Phys. Rev. Lett. **51**, 1888 (1983).

[66] M. Marques, Ph.D. thesis, Bayerische Julius-Maximilians Universität Würzburg, 1998.

[67] F. Essenberger, P. Buczek, A. Ernst, L. Sandratskii, and E. K. U. Gross, Phys. Rev. B **86**, 060412 (2012).

[68] W. L. McMillan, Phys. Rev. **167**, 331 (1968).

[69] P. B. Allen and R. C. Dynes, Phys. Rev. B **12**, 905 (1975).

[70] S. Massidda, F. Bernardini, C. Bersier, A. Continenza, P. Cudazzo, A. Floris, H. Glawe, M. Monni, S. Pittalis, G. Profeta, A. Sanna, S. Sharma, and E. K. U. Gross, Supercond. Sci. Technol. **22**, 034006 (2009).

[71] A. Sanna Ph.D. thesis, Università degli Studi di Cagliari, 2007.

[72] P. Buczek, A. Ernst, P. Bruno, and L. M. Sandratskii, Phys. Rev. Lett. **102**, 247206 (2009).